Journal of Colloid and Interface Science 350 (2010) 402–408

Contents lists available at ScienceDirect

Journal of Colloid and Interface Science

www.elsevier.com/locate/jcis

Spontaneous adsorption of silver nanoparticles on Ti/TiO_2 surfaces. Antibacterial effect on *Pseudomonas aeruginosa*

C.Y. Flores [a], C. Diaz [a], A. Rubert [a], G.A. Benítez [a], M.S. Moreno [b], M.A. Fernández Lorenzo de Mele [a,c], R.C. Salvarezza [a], P.L. Schilardi [a,*], C. Vericat [a,**]

[a] *Instituto de Investigaciones Fisicoquímicas Teóricas y Aplicadas (INIFTA), Facultad de Ciencias Exactas, Universidad Nacional de La Plata – CONICET, Casilla de Correo 16, Sucursal 4, (1900) La Plata, Argentina*
[b] *Departamento de Materiales, Centro Atómico Bariloche, Av. Bustillo Km. 9.5 - (8400) San Carlos de Bariloche, Argentina*
[c] *Facultad de Ingeniería, Universidad Nacional de La Plata, La Plata, Argentina*

ARTICLE INFO

Article history:
Received 18 March 2010
Accepted 19 June 2010
Available online 25 June 2010

Keywords:
Silver nanoparticles
Titanium
Implants
Antibacterial
Pseudomonas aeruginosa

ABSTRACT

Titanium is a corrosion-resistant and biocompatible material widely used in medical and dental implants. Titanium surfaces, however, are prone to bacterial colonization that could lead to infection, inflammation, and finally to implant failure. Silver nanoparticles (AgNPs) have demonstrated an excellent performance as biocides, and thus their integration to titanium surfaces is an attractive strategy to decrease the risk of implant failure. In this work a simple and efficient method is described to modify Ti/TiO_2 surfaces with citrate-capped AgNPs. These nanoparticles spontaneously adsorb on Ti/TiO_2, forming nanometer-sized aggregates consisting of individual AgNPs that homogeneously cover the surface. The modified AgNP–Ti/TiO_2 surface exhibits a good resistance to colonization by *Pseudomonas aeruginosa*, a model system for biofilm formation.

© 2010 Elsevier Inc. All rights reserved.

1. Introduction

Nanotechnology is nowadays having a high impact on almost all areas of biotechnology [1,2] and in medicine [2–5]. In fact, applications of nanotechnology-derived materials, especially of nanoparticles (NPs) of different materials, in areas related to diagnosis and therapeutics, such as pathogen detection [6], drug delivery [7–10], burn healing [11], disease diagnosis [12] and imaging [13,14], among others, are in continuous progress.

On the other hand, one of the most investigated issues in medicine is related to the development of implantable devices that help in the treatment of diverse diseases and in the replacement of parts of the body. The insertion of implants and medical devices has emerged as a common and often life-saving procedure. Titanium has a high strength-to-weight ratio, is resistant to corrosion, biocompatible and has the property to osseointegrate, and these are some of the reasons why it is widely used in orthopedics and dentistry [15,16]. Titanium-made implants have a high performance and durability: for instance, some dental implants can remain in place for over 30 years.

However, one of the most important risk factors of all invasive medical devices is that they predispose to infection [17] by damaging or invading epithelial or mucosal barriers, as well as by supporting the growth of microorganisms by serving as reservoirs. Invasive medical devices impair host defense mechanisms and, when contaminated, can result in resistant chronic infection or tissue necrosis, these being the major objections to the extended use of implant devices [18]. Thus, biomaterial implant-related infections remain as one of the main causes of implant failures [18,19].

Either as ionic species or colloidal particles, silver has been used as an antimicrobial agent for years [20], long before the appearance of antibiotics. Silver materials have some advantages with respect to antibiotics: unlike them they show antibacterial effect against all bacteria and they do not present the problem of developing resistance (as it does happen with antibiotics).

In particular, silver nanoparticles (AgNPs) have excellent biocidal properties [21–25], although their mechanism of action is not yet completely understood [26,27]. Several methods of synthesis, such as chemical reduction in aqueous and non aqueous solvents, photochemical reduction and sol–gel methods can be used to prepare stable AgNPs [28]. It has been demonstrated that silver nanoparticles retain their bactericidal properties [28–30] when included in coatings [31,32]; bandages for burn healing [33], and dressing materials for wound repair [34], among others. Therefore, they can be included as coating on orthopedic and other implantable devices [31,35,36].

* Corresponding author. Fax: +54 221 4254642.
** Corresponding author. Fax: +54 221 4254642.
E-mail addresses: pls@inifta.unlp.edu.ar, pls@quimica.unlp.edu.ar (P.L. Schilardi), cvericat@inifta.unlp.edu.ar (C. Vericat).

0021-9797/$ - see front matter © 2010 Elsevier Inc. All rights reserved.
doi:10.1016/j.jcis.2010.06.052

Since bacterial infections associated with titanium implants remain a major cause of their failure [37], considerable interest has arisen in the preparation and study of the properties (both physical–chemical and antibacterial) of Ti/TiO_2 surfaces modified with silver [38–41]. Several strategies have been used for their preparation, including the complexation of Ag^+ ions with mercaptan-terminated phosphonates [41], silver sputtering [38], adsorption of nanoparticles on amine-terminated silane monolayers [42], the use of silver and hydroxyapatite/TiO_2 slurries [43], and sol–gel procedures [40,44], among others. It has been reported that these modified surfaces are biologically compatible [37,45] and present antimicrobial activity [46]. Moreover, in some cases it has been demonstrated that they present visible light photocatalysis [47].

The aim of this paper is to report a simple and easy method to modify Ti/TiO_2 surfaces with citrate-capped AgNPs by spontaneous adsorption. To the best of our knowledge, this simple method – which does not need the preparation of a monolayer of organic molecules (phosphonate, silane, etc.) on the Ti/TiO_2 surface as a previous step, or any heating procedures – has not been previously reported in public literature. The antimicrobial effect of the modified surfaces has been tested against *Pseudomonas aeruginosa* (*P. aeruginosa*), an opportunistic microorganism that can cause severe, life-threatening infections and is primarily a nosocomial pathogen [48].

This easy method of adsorbing AgNPs (and other nanoparticles) from solution can be used to modify not only Ti/TiO_2 surfaces of implants but also other surfaces (as long as they have an oxide layer) that need to be in contact with a biologically active environment and which are also plausible of biofilm development. The strategy can also be applied to prepare catalysts such as those consisting of gold nanoparticles [49] (capped with carboxylic acids) on TiO_2 and other oxides [50], which have been found to be effective to catalyze important reactions. Finally, it may also be interesting to assess the possibility of using TiO_2 and other oxide surfaces to recover residual metallic nanoparticles from water, an important issue for environmental decontamination.

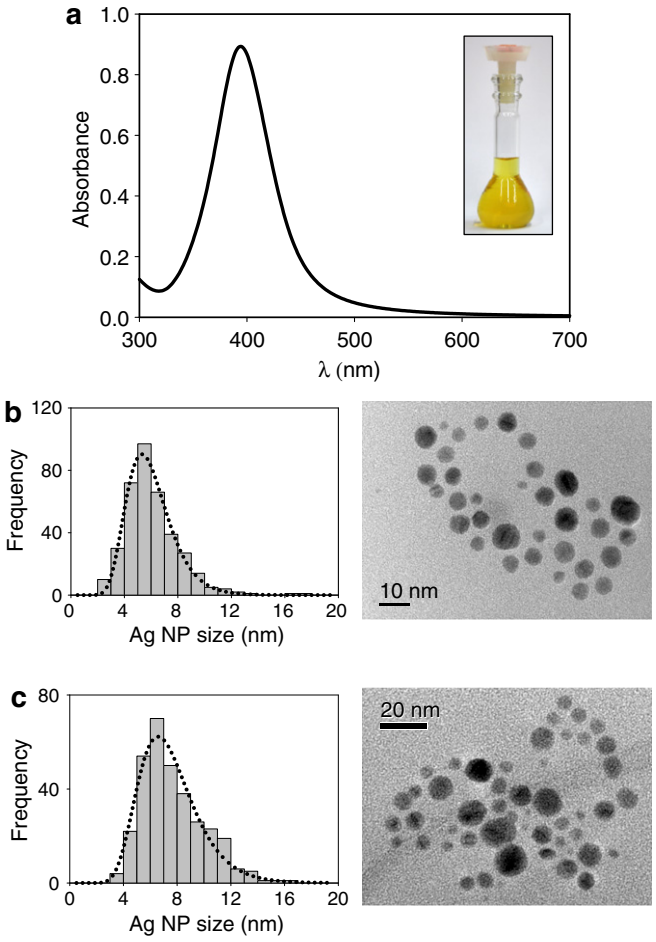

Fig. 1. (a) UV vis spectrum (1 in 4 dilution of the original solution). Inset: picture of the original AgNP solution. (b) and (c) TEM imaging of silver nanoparticles: (b) fresh nanoparticles: (left) histogram showing the size distribution of the AgNPs. The dotted line corresponds to the fitted log-normal distribution; (right) TEM image showing individual nanoparticles. (c) Nanoparticles three weeks after the synthesis: (left) histogram showing the size of the AgNPs. The dotted line corresponds to the fitted log-normal distribution; (right) TEM image showing individual nanoparticles.

2. Experimental

2.1. Silver nanoparticle preparation

Silver nanoparticles in aqueous solution were prepared by reduction of $AgNO_3$ with $NaBH_4$ and stabilized by using trisodium citrate. All reagents used in the synthesis were of analytical grade and solutions were prepared with Milli Q water (18 MΩ cm). Briefly, 1 mL of a 5 mM aqueous $AgNO_3$ solution was added to 16 mL of a 1.06 mM aqueous sodium citrate solution under magnetic stirring in an ice/water bath at around 0 °C. Then, 100 μL of a freshly prepared 100 mM aqueous $NaBH_4$ solution were added dropwise over 5 min. The initially colorless solution became yellow and was stirred at around 0 °C for 1 h and 45 min. The final Ag concentration in the nanoparticle solution is 3.16×10^{-2} mg Ag/mL. The nanoparticles obtained hereby are stable for weeks. A picture of the final solution is shown in the inset in Fig. 1a.

2.2. Characterization of AgNPs

UV–vis spectra of the nanoparticles (1:4 dilutions of the original solutions, 7.9×10^{-3} mg Ag/mL) were acquired with a Lambda 35 double beam spectrophotometer from Perkin Elmer (Waltham, MA, USA).

As-prepared citrate-capped AgNPs were characterized by Transmission Electron Microscopy (TEM) using a Philips CM200 UT microscope operating at 200 kV and room temperature.

2.3. Immobilization of AgNPs on Ti/TiO_2 surfaces

Titanium foils (99.7%, 0.25 mm thickness, obtained from Johnson-Mathey) were first polished with abrasive paper, sonicated for 45 min, and then polished at mirror grade with 1 μm diamond paste, further sonicated for 45 min, thoroughly rinsed and dried. The freshly polished Ti substrates were incubated in the as-prepared AgNP solutions (3.16×10^{-2} mg Ag/mL) in the dark at 4 °C for 24 h. The used solutions had been synthesized 1–3 weeks prior to their use for Ti substrate incubation, and therefore show some aging. For some AFM measurements the incubation was made for only 45 min in the same solutions.

To assess the role of the citrate capping some Ti foils were modified with AgNPs whose citrate capping had been replaced by polysorbates (Tween 20™) by a modification of a procedure reported for gold nanoparticles [51]. The concentration of the citrate and polysorbate-capped AgNPs solution used for the 24 h incubation was the same, and the modified substrates were analyzed by XPS.

2.4. Characterization of AgNPs on Ti/TiO_2

X-ray Photoelectron Spectroscopy (XPS) measurements of the silver nanoparticles immobilized on Ti/TiO_2 were performed using

a Mg Kα source (XR50, Specs GmbH) and a hemispherical electron energy analyzer (PHOIBOS 100, Specs GmbH) operating at 10 eV pass energy. A two-point calibration of the energy scale was performed using sputtered cleaned gold (Au $4f_{7/2}$, binding energy = 84.00 eV) and copper (Cu $2p_{3/2}$, binding energy = 933.67 eV) samples. C 1s at 285 eV was used as charging reference. Spectra were analyzed with CasaXPS v2.3.14 and XPS Peak 4.0 software packages. The fitting of the Ag 3d peaks was carried out using a spin–orbit splitting of 6.01 eV and a branching ratio of 0.66, after subtracting a Shirley type background.

Atomic Force Microscopy (AFM) imaging of the different samples was done in air in the contact mode with a Contact AFM commanded by a Nanoscope IIIa control unit from Veeco Instruments (Santa Barbara, CA, USA). Triangular silicon nitride probes (k = 0.58 N/m) from Veeco Instruments (Santa Barbara, CA, USA) were used in all measurements. These tips have been chosen in order to use the same probes both for AgNP and bacteria imaging. Exerted forces were in the order of 4 nN, as calculated from experimental force curves and force constant measurements employing the thermal noise method. In some cases the tip shape changed with scanning time and after some time the imaged AgNP aggregates were seen to have a rectangular shape (tip artifact). Therefore, care was taken to use new tips for each imaged region.

2.5. Growth conditions and AFM imaging of bacteria

P. aeruginosa (from clinic isolation) was inoculated in 150 mL of sterile liquid nutrient broth (Merck) and grown for 24 h at 30 °C in soft agitation. The microbial concentration was 10^{10}–10^{11} CFU/mL, according to optical density measurements by UV–visible spectroscopy at 586 nm. After that, appropriate dilutions were made in order to reach the desired bacterial concentration.

For AFM imaging of bacteria attached to the surfaces, the substrate was incubated for 4 h in broth ($\sim 10^{10}$ CFU/mL), gently rinsed with sterile water and dried in air. The conditions for AFM imaging were similar to those described above for AgNP-modified substrates.

2.6. Viability of bacteria attached to Ti/TiO_2 surfaces

2.6.1. Bacteria growing halo assays

Titanium substrates (both control and modified with silver NPs) were each exposed to a *P. aeruginosa* culture ($\sim 4 \times 10^9$ CFU/mL) for 4 h in order to allow bacteria adhesion to the TiO_2 surface. Then the substrates were rinsed with sterile water to remove non-attached cells. Subsequently, they were placed on plates with sterile nutrient agar (Merck) for 24 h at 30 °C. Under these conditions some bacteria from the substrates move towards the agar surface and begin to grow on the surrounding area. Formation of the growing halo was studied. Each experiment was repeated at least three times.

2.6.2. Quantitative viability assays

Assays were carried out by using the LIVE/DEAD BacLight® viability kit (Invitrogen). The live/dead kit includes the green fluorescent DNA-binding stain SYTO 9 and the red fluorescent DNA-binding stain propidium iodide (PI), enabling the determination of bacterial viability from the difference in membrane integrity in embedded cells. When used alone, the SYTO-9 stain generally labels all bacteria in a population, whereas propidium iodide penetrates only bacteria with damaged membranes, causing a reduction in the SYTO-9 stain. The live/dead stain was prepared by mixing 30 μL of staining component A (SYTO 9) and 30 μL of staining component B (propidium iodide) and diluting the mixture to 1/200 in distilled water. Ten microliters of the dye was poured on each substrate and then they were kept in the dark for 15 min at room temperature. After that, the substrates were rinsed with sterile H_2O. Stained bacteria were visualized by epifluorescence with an Olympus BX-51 microscope. The microscope filters used were U-MWG2 (excitation 510–550 nm and emission 590 nm) and U-MWB2 (excitation 460–490 nm and emission 520 nm).

Bacterial viability was calculated from the ratio of the number of intact cells stained with SYTO-9 to the total number of cells (intact plus propidium iodine-positive (damaged) cells). Calculations were made with images from at least 10 randomly selected regions.

3. Results and discussion

3.1. Characterization of AgNPs nanoparticles

In Fig. 1a, a UV–vis spectrum of the freshly synthesized silver nanoparticles (1:4 dilution) is shown. The typical surface plasmon absorption peak can be observed at ≈400 nm. After several weeks the AgNPs yield similar spectra, an indication of the fact that they are stable with time. TEM imaging of the fresh, as-prepared AgNP solution (Fig. 1b) reveals that the nanoparticles are not aggregated. The nanoparticle size distribution can be fitted with a log-normal function centered at 6 nm (histogram in Fig. 1b). TEM images of AgNPs studied after a 3 week aging show that nanoparticles do not aggregate (Fig. 1c) and also that some of the nanoparticles slightly increase their size. The size distribution cannot be well-fitted with a log-normal function (histogram in Fig. 1c), a fact that can be attributed to coarsening. However, even 1 year after the synthesis, nanoparticle size distributions are similar to those shown in Fig. 1c. In all cases the position of the plasmon absorption peak for the nanoparticles is consistent with the size range observed, as determined from TEM (Fig. 1b and c) and AFM data (see below) [52].

3.2. AgNP adsorption on Ti surfaces

First, we will demonstrate that AgNPs can spontaneously adsorb on the Ti surface. It should be noted that the titanium surface is always covered by a native oxide film owing to its spontaneous passivation [39], and therefore we will refer to the surface as Ti/TiO_2. In Fig. 2a, a typical XPS survey of the Ti/TiO_2 surface after immersion for 24 h in a AgNP colloidal solution is shown. The survey shows the Ti, O, Ag and C signals, indicating that the citrate-capped AgNPs are adsorbed on the Ti/TiO_2 surface. The Ag/Ti intensity ratio (corrected by the sensitivity factors) calculated from low resolution scans for Ag 3d and Ti 2p is 0.12 ± 0.03.

High resolution XPS spectra of the Ti 2p and Ag 3d regions are shown in Fig. 2b and c, respectively. The Ti $2p_{3/2}$ peak has a maximum at ≈459 eV (Fig. 2b) which can be assigned to a single species: the native TiO_2 which, as mentioned before, is spontaneously formed on the surface due to the presence of oxygen in air and in water (BE = 458.5 eV) [53]. The spin–orbit splitting is 5.8 eV, in agreement with what is reported for TiO_2 [53]. There is no contribution from metallic Ti (BE = 453.8 eV) [53], which is reasonable considering the expected thickness of the native oxide (8 nm in air [54], and maybe even more in aqueous solutions) and the fact that photoelectrons from a buried Ti layer can be detected only if the oxide overlayer is thinner than 6 nm.

In the case of Ag 3d (Fig. 2c), the spectrum can be fitted with a single component with $3d_{5/2}$ BE at 368.3 eV (FWHM = 1 eV), which has been assigned to metallic silver [55]. The nanoparticles are not oxidized, as no further components at lower BE energy are needed for the fit. This has been corroborated by selected area electron diffraction and HRTEM images, which are consistent with a cubic metallic Ag lattice. Moreover, AgNPs remain mostly metallic after several months, as revealed by XPS and TEM (data not shown).

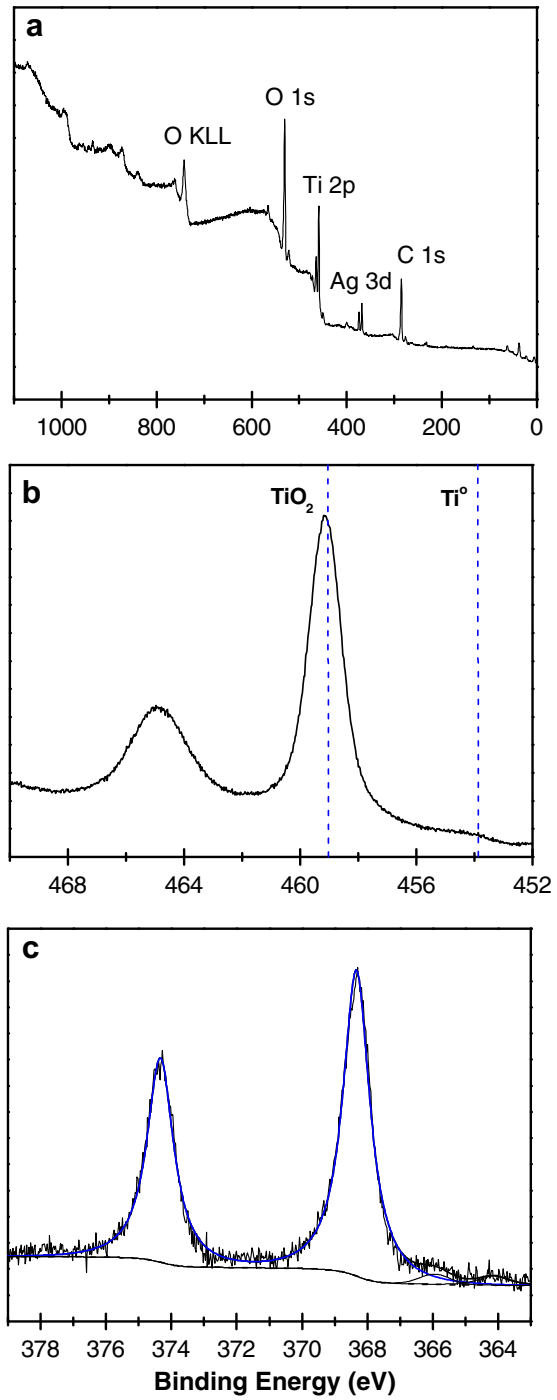

Fig. 2. XPS spectra. (a) Survey. (b) High resolution Ti 2p. The titanium surface is completely oxidized. (c) High resolution Ag 3d. The spectrum can be fitted with a single component corresponding to metallic silver.

These results clearly demonstrate that citrate-capped AgNPs spontaneously adsorb on Ti/TiO_2 surfaces. In the following, we will refer to the spatial distribution of the adsorbed AgNPs on Ti/TiO_2 surfaces (Fig. 3). Fig. 3a and b shows typical contact AFM images taken in air of polished titanium foils which have been immersed in silver nanoparticle-containing solutions for 24 h. The AgNP solutions were used 1–3 weeks after the synthesis. The Ti/TiO_2 surfaces exhibit homogeneously distributed islands 100–300 nm in size (bright spots in the images). Each island presumably consists of many silver nanoparticles. In fact, Ti/TiO_2 surfaces not exposed to silver nanoparticles do not show the aggregates (data not shown). From the analysis of cross sections of the AFM images (Fig. 3d) the height of the AgNP islands can be estimated to be 80 ± 40 nm (i.e., they are formed by several layers of AgNPs). In some cases some scratches can be observed due to the polishing process (Fig. 3a, bottom right).

The surface coverage of the islands (calculated with the "Bearing" Nanoscope software tool) is 0.09 ± 0.03. On the other hand, from the intensity ratio of the Ag 3d and Ti 2p XPS peaks, and considering the height of the aggregates obtained from AFM images, a surface coverage of Ag islands on TiO_2 of 0.09 ± 0.02 can be estimated. For this estimation the effective attenuation lengths for the Ag 3d electrons on Ag, and Ti 2p electrons on Ag and on TiO_2 were extracted from the NIST database [56]. Therefore, there is agreement between AFM (local technique) and XPS (average technique) as regards the Ag island coverage after 24 h.

In order to elucidate the structure of the aggregates we have prepared Ti/TiO_2 samples incubated in AgNP solutions for shorter times. For incubation times of 45 min it can be seen that aggregates do not fully cover the titanium surface. The regions covered by AgNPs show smaller aggregates than for 24 h (Fig. 2c). Moreover, some lines can be seen in the image due to the fact that, although care was taken to use low applied forces in the repulsive regime, the tip removes a few loosely attached nanoparticles from the islands while scanning the sample. More important, a detailed analysis of some of the islands reveals that they are formed by individual citrate-capped AgNPs (Fig. 3c).

In fact, from cross section analysis, interesting information can be obtained about the size of adsorbed nanoparticles (Fig. 3e). Assuming that the tip and the AgNPs have similar radii (and considering spherical nanoparticles, as revealed by TEM), it is possible to roughly estimate the size of the adsorbed individual NPs by using the equation $r_c = 2\sqrt{(Rr)}$ [57], where r_c is the measured radius, and R and r are the tip and individual NP radii, respectively. If we consider $r_c = 20$ nm (as obtained from Fig. 3e), then the size of individual NPs is about 10 nm, in reasonable agreement with TEM results, considering that AFM also measures the citrate capping (≈1 nm), and that there is some aging of the employed AgNPs (Fig. 1c). This is also the height obtained from the cross sections in Fig. 3e. Therefore from our results we can conclude that the aggregates consist of individual AgNPs, as reported for thiol-capped AuNPs spontaneously adsorbed on HOPG [58], which do not show significant Ostwald ripening once on the surface.

Evidently, the stability of the 3D aggregates is relatively strong, since they can be imaged by contact AFM without removing them with the tip by using relatively soft cantilevers and low applied forces. As regards the possible interactions involved in the formation of AgNP aggregates on the surface, it is clear that the adsorption of NPs and the formation of aggregates should be influenced both by nanoparticle-TiO_2 surface and nanoparticle–nanoparticle interactions.

From AFM images it is clear that after 24 h the formed aggregates are one order of magnitude wider than higher (see Fig. 3b and d), which implies that AgNP–TiO_2 surface interactions are stronger than nanoparticle–nanoparticle interactions. While the contribution of van der Waals interactions [59] cannot be disregarded, it is well-known that carboxylic acids adsorb on oxide-covered surfaces [60,61]. In particular, it has been proposed that carboxylic acids form surface complexes on oxidized titanium surfaces [62]. This strong interaction could be responsible for the high stability of our citrate-capped AgNPs on the oxidized titanium surface. In fact, XPS data of Ti/TiO_2 immersed in a citrate solution shows the typical C 1s signal at 289 eV assigned to carboxylate species (Fig. 4), indicating that these ions spontaneously adsorb on the oxide surface. We have performed additional XPS measurements with Ti/TiO_2 modified with AgNPs whose citrate capping has been

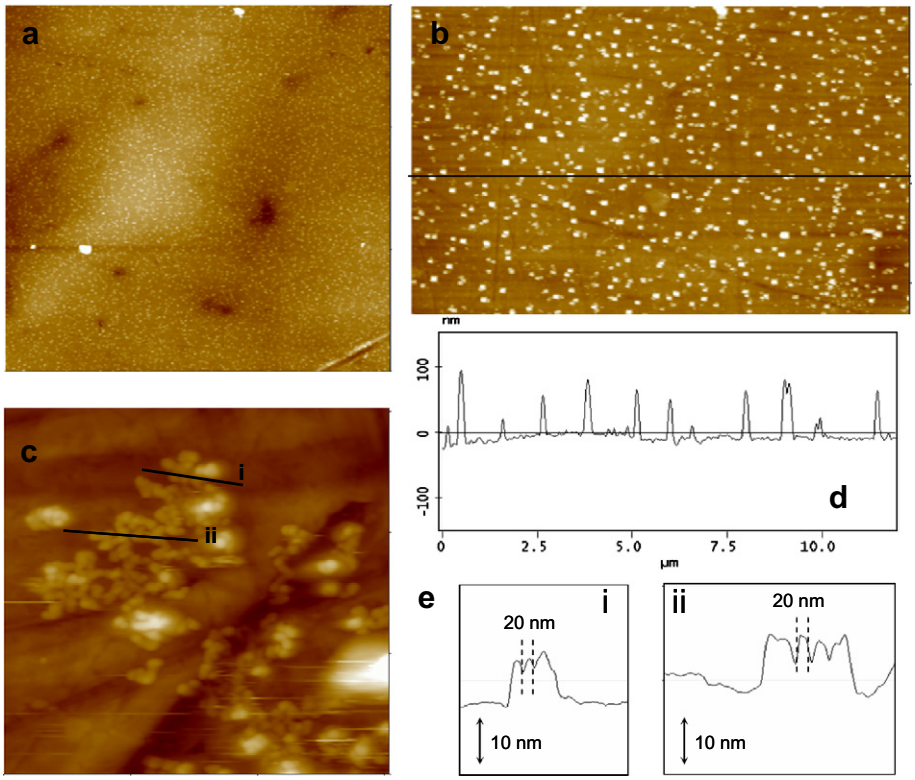

Fig. 3. In air contact AFM images of AgNP-modified titanium substrates. (a) 30 × 30 μm^2 and (b) 12 × 7.4 μm^2: the nanoparticle aggregates entirely cover the Ti surface after 24 h incubation. (c) High resolution AFM image (760 × 760 nm^2): individual AgNP can be clearly observed after 45 min incubation. (d) Cross section of (b) showing the height of the NP aggregates. (e) Cross sections (i and ii) of (c) showing the measured size and height of the individual nanoparticles.

replaced by a polysorbate coating and have compared the results with those of citrate-capped AgNPs (both nanoparticle solutions had the same concentration). What we found is that the Ag/Ti ratio is always larger for citrate-capped AgNPs (approximately seven times larger). Thus, it is reasonable to attribute the AgNP–TiO_2 surface interaction to the citrate capping.

Since the height of the islands as imaged by AFM involves several nanoparticle layers, it is evident that also nanoparticle–nanoparticle interactions are involved in island stabilization. In this case we can speculate that, in addition to the contribution of van der Waals forces between citrate chains (as it has been proposed for adsorption of gold nanoparticles on HOPG [58]) hydrogen bonds should play a role in the formation of the AgNP aggregates. In fact, in the case of superlattices of carboxylic acid-capped gold nanoparticles, hydrogen bonds have been proposed as the controlling interaction between the particle and the mediator that regulates interparticle spacing [63].

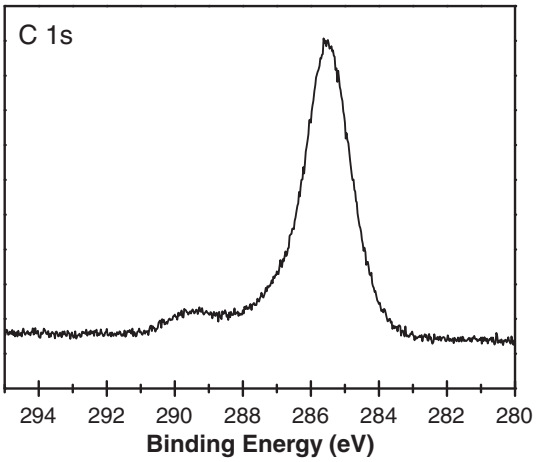

Fig. 4. High resolution XPS C 1s spectrum of a Ti/TiO_2 surface immersed in a 17 mM citrate solution for 24 h. The small peak centered at ≈289 eV corresponds to carboxylate species.

From combined XPS and AFM data we have determined that after 24 h the spontaneous adsorption of citrate-capped AgNPs results in the formation of 3D nanoparticle islands homogeneously distributed on the Ti/TiO_2 surface. Although several other methods have been previously reported in the literature to modify titanium or titanium dioxide surfaces with silver [41,64,65], ours is cheap, straightforward and yields a surface homogeneously covered by AgNP islands with very little effort. This strategy can thus be applied to modify Ti implant surfaces with no need for expensive equipment or trained specialists.

3.3. Study of the antibacterial effect of the AgNP-modified substrates

We have employed a *P. aeruginosa* strain to study the biocide activity of the AgNP-modified titanium substrates. *P. aeruginosa* is a Gram-negative bacterium and is considered a model for biofilm formation and pathogenesis [66]. In fact, *P. aeruginosa* exude an important amount of extracellular polymeric material (EPM) which can in part protect them from the bactericidal action of silver-modified surfaces. In addition, *P. aeruginosa* is an opportunistic microorganism that can cause severe, life-threatening infections and is primarily a nosocomial pathogen [48]. While it rarely causes disease in healthy persons, it can cause urinary tract infections, respiratory system infections and a variety of systemic infection in immunosuppressed patients.

Fig. 5 shows in air AFM images of bacteria attached on control (without AgNPs, Fig. 5a) and AgNP-modified Ti/TiO_2 surfaces

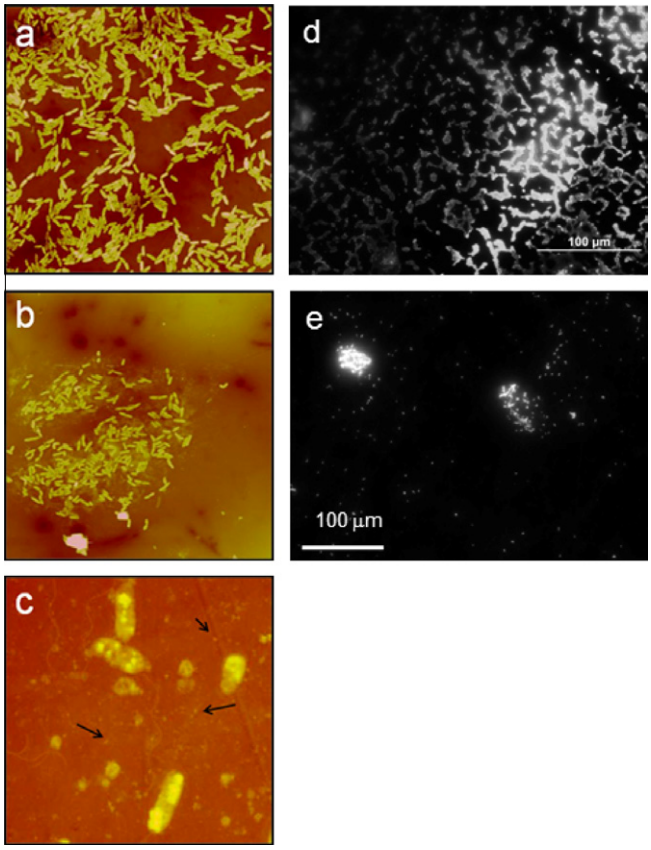

Fig. 5. Images of *P. aeruginosa* (4 h incubation) attached on (a) control surface (unfiltered AFM image, 50×50 μm^2), (b) NP-modified surface (unfiltered AFM image, 50×50 μm^2), (c) NP-modified surface after 72 h exposure to bacteria culture showing AgNP aggregates (arrows) (higher resolution unfiltered AFM image, 8×8 μm^2), (d) control surface (optical image) and (e) NP-modified surface (optical image).

(Fig. 5b) after 4 h of incubation in nutrient broth. Qualitative inspection of the images shows that the number of attached bacteria on control surfaces is greater than that found for AgNP-modified substrates. This fact was confirmed by optical microscopy imaging of the cells (Fig. 5d and e). EPM seems to form a physical barrier between the modified substrate and cells, in order to avoid contact with toxic AgNPs. Similar biofilm structure and EPM production has been previously reported for *Pseudomonas fluorescens* biofilms on copper surfaces as a response to toxic copper products of corrosion [67]. It should be noted that the resulting biofilm is formed

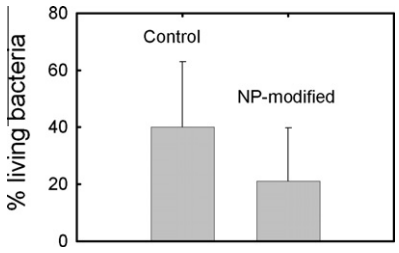

Fig. 7. Percentage of viable bacteria on control and on AgNP-modified surfaces.

both by both, bacteria from the broth and from duplication of the cells attached to the substrate (daughter cells). Interestingly, the nanoparticle aggregates remain adsorbed on the Ti/TiO_2 surfaces (small bright spots, see arrows, in Fig. 5c) even after having been exposed to aqueous media for long periods of time (more than 72 h), as it can be observed in the AFM image showed in Fig. 5c.

As it has been previously reported [68], the investigation of the antimicrobial activity of surfaces containing silver as a biocidal agent is difficult because many silver compounds have low solubility in water, resulting in low concentrations of silver ions released into the surrounding medium. Thus, routine agar diffusion measurements tests (such as the Kirby–Bauer test) are not suitable for that purpose.

We have therefore tested the efficiency as antimicrobial coating of AgNP on Ti/TiO_2 surfaces by checking the ability of attached bacteria to form colonies in agar. Bacteria attached to a surface are able to duplicate, move and form colonies beyond the biofilm. Bacteria from the biofilm formed on the Ti/TiO_2 surface move and colonize the surrounding agar area forming a halo. From growing halo assays it is possible to have an indication about the viability of the bacteria attached to the surface. Fig. 6 shows bacterial spreading on agar plates from early stages of biofilm formation on AgNP-modified (Fig. 6a) and on control (Fig. 6b) Ti/TiO_2 substrates after 24 h incubation in nutrient agar. The measured values are 0.28 cm for the AgNP-covered substrate and 1.24 cm for the control substrate (Fig. 6). These results confirm that there are less viable cells attached on AgNP-covered surface than on the control. Additionally, the diffusion of silver ions from the AgNP-covered substrate could also inhibit the growth of bacteria on the agar in the vicinity of this substrate, reducing the halo area.

In order to obtain some quantitative information about the effectiveness of our AgNP-modified Ti/TiO_2 surfaces, we have carried out viability assays with the LIVE/DEAD BacLight® viability kit. Fig. 7 shows that the number of viable bacteria on AgNP-modified surfaces is smaller compared to those attached to control sur-

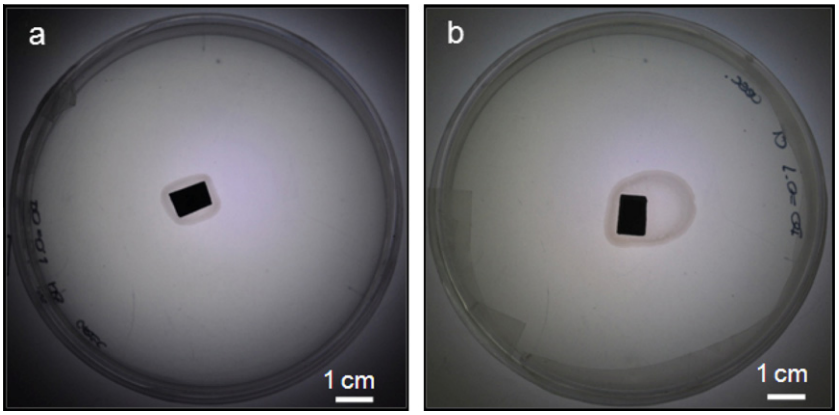

Fig. 6. Growing halo of *P. aeruginosa* coming from the surfaces after 24 h incubation in nutrient agar. (a) AgNP-modified Ti/TiO_2 substrate. (b) Control Ti/TiO_2 (no AgNPs).

faces. Moreover, the number of total cells (live and dead) found on AgNP-modified surfaces represents only a 20 % of those attached to control substrates (see Fig. 5d and e). Therefore, AgNPs on the titanium surface are effective to hinder bacterial adhesion, also reducing the viability of the cells.

4. Conclusions

A simple, low cost and efficient method of modifying Ti/TiO_2 surface with citrate-capped NPs is described and its biocidal efficacy is demonstrated. Stable silver nanoparticles were synthesized, which can be spontaneously adsorbed on Ti/TiO_2 surfaces and are stable on the surface after long periods of exposition to aqueous medium. Citrate capping plays an important role in the interaction of the AgNP with the TiO_2 surface. The AgNP-modified surfaces are efficient for bacteria growth inhibition and suitable for protecting Ti surfaces of implants against pathogen colonization. The preparation of such AgNP-modified surfaces does not require expensive equipment or trained lab specialists. This easy method for modification of Ti/TiO_2 surfaces could be also used to modify other oxide surfaces with these or other nanoparticles, with interesting potential applications.

Acknowledgments

This work has been supported by the ANPCyT (PICT 06-621, PICT 05-33225, PICT 05-32906, PICT 05-32439, PAE 22771), UNLP (Projects 11/X532 and 11/I129), and CONICET (PIP112-200801-00362). C.Y.F. gratefully acknowledges a doctoral fellowship from ANPCyT.

References

[1] J. Gao, B. Xu, Nano Today 4 (1) (2009) 37–51.
[2] S.D. Caruthers, S.A. Wickline, G.M. Lanza, Curr. Opin. Biotechnol. 18 (1) (2007) 26–30.
[3] O.C. Farokhzad, R. Langer, Adv. Drug Delivery Rev. 58 (14) (2006) 1456–1459.
[4] S.K. Sahoo, S. Parveen, J.J. Panda, Nanomedicine: Nanotechnology, Biology and Medicine 3 (1) (2007) 20–31.
[5] C.S.S.R. Kumar, J. Hormes, C. Leuschner, Nanofabrication towards Biomedical Applications, Wiley-VCH Verlag GmbH & Co., KGaA, 2005.
[6] J.D. Driskell, R.A. Tripp, Clin. Microbiol. Newslett. 31 (18) (2009) 137–144.
[7] C. Kim, P. Ghosh, V.M. Rotello, Nanoscale 1 (2009) 61–68.
[8] C.J. Sunderland, M. Steiert, J.E. Talmadge, A.M. Derfus, S.E. Barry, Drug Dev. Res. 67 (1) (2006) 70–93.
[9] J. Dobson, Drug Dev. Res. 67 (1) (2006) 55–60.
[10] S. Mallidi, T. Larson, J. Tam, P.P. Joshi, A. Karpiouk, K. Sokolov, S. Emelianov, Nano Lett. 9 (8) (2009) 2825–2831.
[11] M. Hromadka, J.B. Collins, C. Reed, L. Han, K.K. Kolappa, B.A. Cairns, T. Andrady, J.A. Van Aalst, J. Burn Care Res. 29 (5) (2008) 695–703.
[12] P.V. Baptista, Curr. Cancer Ther. Rev. 5 (2) (2009) 80–88.
[13] D.P. Cormode, T. Skajaa, Z.A. Fayad, W.J.M. Mulder, Arterioscler., Thromb., Vasc. Biol. 29 (7) (2009) 992–1000.
[14] D. Pan, G.M. Lanza, S.A. Wickline, S.D. Caruthers, Eur. J. Radiol. 70 (2) (2009) 274–285.
[15] R. Van Noort, J. Mater. Sci. 22 (11) (1987) 3801–3811.
[16] O.E.M. Pohler, Injury 31 (Suppl. 4) (2000) D7–D13.
[17] J.M. Schierholz, J. Beuth, J. Hospital Infect. 49 (2001) 87–93.
[18] L. Zhao, P.K. Chu, Y. Zhang, Z. Wu, J. Biomed. Mater. Res. Part B: Appl. Biomater. 91B (1) (2009) 470–480.
[19] A. Trampuz, F. Widmer, Curr. Opin. Infect. Dis. 19 (2006) 349–356.
[20] I. Chopra, J. Antimicrob. Chemother. 59 (4) (2007) 587–590.
[21] A. Petica, S. Gavriliu, M. Lungu, N. Buruntea, C. Panzaru, Mater. Sci. Eng., B 152 (1–3) (2008) 22–27.
[22] C. Gunawan, W.Y. Teoh, C.P. Marquis, J. Lifia, R. Amal, Small 5 (3) (2009) 341–344.
[23] E.J. Fernandez, J. Garcia-Barrasa, A. Laguna, J.M. Lopez-de-Luzuriaga, M. Monje, C. Torres, Nanotechnology 19 (18) (2008) 185602.
[24] J.R. Morones, J.L. Elechiguerra, A. Camacho, K. Holt, J.B. Kouri, J.T. Ramirez, M.J. Yacaman, Nanotechnology 16 (10) (2005) 2346–2353.
[25] K. Vasilev, V. Sah, K. Anselme, C. Ndi, M. Mateescu, B.r. Dollmann, P. Martinek, H. Ys, L. Ploux, H.J. Griesser, Nano Lett. 10 (1) (2009) 202–207.
[26] E.T. Hwang, J.H. Lee, Y.J. Chae, Y.S. Kim, B.C. Kim, B.I. Sang, M.B. Gu, Small 4 (6) (2008) 746–750.
[27] S. Shrivastava, T. Bera, A. Roy, G. Singh, P. Ramachandrarao, D. Dash, Nanotechnology 18 (22) (2007) 225103.
[28] V.K. Sharma, R.A. Yngard, Y. Lin, Adv. Colloid Interface Sci. 145 (1–2) (2009) 83–96.
[29] R. Vaidyanathan, K. Kalishwaralal, S. Gopalram, S. Gurunathan, Biotechnol. Adv., in press (corrected proof).
[30] L. Kvitek, A. PanacÌŒek, J. Soukupova, M. Kolar, R. VecÌŒerova, R. Prucek, M. Holecova, R. Zboril, J. Phys. Chem. C 112 (15) (2008) 5825–5834.
[31] K.N.J. Stevens, O. Crespo-Biel, E.E.M. van den Bosch, A.A. Dias, M.L.W. Knetsch, Y.B.J. Aldenhoff, F.H. van der Veen, J.G. Maessen, E.E. Stobberingh, L.H. Koole, Biomaterials 30 (22) (2009) 3682–3690.
[32] K. Vasilev, V. Sah, K. Anselme, C. Ndi, M. Mateescu, B.r. Dollmann, P. Martinek, H. Ys, L. Ploux, H.J. Griesser, Nano Lett. 10 (1) (2010) 202–207.
[33] R. Jung, Y. Kim, H.S. Kim, H.J. Jin, J. Biomater. Sci., Polym. Ed. 20 (3) (2009) 311–324.
[34] S.A. Jones, P.G. Bowler, M. Walker, D. Parsons, Wound Repair Regen. 12 (3) (2004) 288–294.
[35] L.S. Nair, C.T. Laurencin, J. Bone Joint Surg. – Ser. A 90 (Suppl. 1) (2008) 128–131.
[36] D.R. Monteiro, L.F. Gorup, A.S. Takamiya, A.C. Ruvollo-Filho, E.R.d. Camargo, D.B. Barbosa, Int. J. Antimicrob. Agents 34 (2) (2009) 103–110.
[37] L. Zhao, P.K. Chu, Y. Zhang, Z. Wu, J. Biomed. Mater. Res. – Part B Appl. Biomater. 91 (1) (2009) 470–480.
[38] A.R. Canário, E.A. Sanchez, Y. Bandurin, V.A. Esaulov, Surf. Sci. 547 (3) (2003) L887–L894.
[39] S. Schroth, M. Schneider, T. Mayer-Uhma, A. Michaelis, V. Klemm, Surf. Interface Anal. 40 (3–4) (2008) 850–852.
[40] J. Thiel, L. Pakstis, S. Buzby, M. Raffi, C. Ni, D.J. Pochan, S.I. Shah, Small 3 (5) (2007) 799–803.
[41] J. Amalric, P.H. Mutin, G. Guerrero, A. Ponche, A. Sotto, J.P. Lavigne, J. Mater. Chem. 19 (1) (2009) 141–149.
[42] L. Juan, Z. Zhimin, M. Anchun, L. Lei, Z. Jingchao, Int. J. Nanomed. 5 (1) (2010) 261–267.
[43] A. Mo, J. Liao, W. Xu, S. Xian, Y. Li, S. Bai, Appl. Surf. Sci. 255 (2) (2008) 435–438.
[44] O. Akhavan, J. Colloid Interface Sci. 336 (1) (2009) 117–124.
[45] K. Das, S. Bose, A. Bandyopadhyay, B. Karandikar, B.L. Gibbins, J. Biomed. Mater. Res. – Part B Appl. Biomater. 87 (2) (2008) 455–460.
[46] M. Sokmen, S. Degerli, A. Aslan, Exp. Parasitol. 119 (1) (2008) 44–48.
[47] J. Zheng, H. Yu, X. Li, S. Zhang, Appl. Surf. Sci. 254 (6) (2008) 1630–1635.
[48] Y. Gulay, O. Baris, C. Aysegul, K. Cigdem, D. Riza, Am. J. Infect. Control 34 (4) (2006) 188–192.
[49] D.T. Thompson, Nano Today 2 (4) (2007) 40–43.
[50] H. Hartshorn, C.J. Pursell, B.D. Chandler, J. Phys. Chem. C 113 (24) (2009) 10718–10725.
[51] K. Aslan, V.H. Perez-Luna, Langmuir 18 (16) (2002) 6059–6065.
[52] D.D.E. Evanoff, G. Chumanov Jr., ChemPhysChem 6 (7) (2005) 1221–1231.
[53] C.D. Wagner, W.M. Riggs, L.E. Davis, J.F. Moulder, G.E. Mullenberg, Handbook of X-ray Photoelectron Spectroscopy, Perkin–Elmer Corp., 1979.
[54] E. McCafferty, J.P. Wightman, Appl. Surf. Sci. 143 (1–4) (1999) 92–100.
[55] G.I.N. Waterhouse, G.A. Bowmaker, J.B. Metson, Appl. Surf. Sci. 183 (3–4) (2001) 191–204.
[56] C.J. Powell, A. Jablonski, National Institute of Standards and Technology, Gaithersburg, MD, 2003.
[57] http://www.ntmdt.com/spm-basics/view/effect-tip-radius-cone-angle.
[58] D. Grumelli, C. Vericat, G. Benitez, M.E. Vela, R.C. Salvarezza, L.J. Giovanetti, J.M. Ramallo-Lopez, F.G. Requejo, A.F. Craievich, Y.S. Shon, J. Phys. Chem. C 111 (19) (2007) 7179–7184.
[59] J.N. Israelachvili, Intermolecular and Surface Forces, Academic Press, 1992.
[60] H. Onishi, in: Springer Series in Chemical Physics, vol. 70, 2003, pp. 75–89.
[61] A. Sasahara, H. Uetsuka, H. Onishi, Surf. Sci. 481 (1–3) (2001) L437–L442.
[62] A.D. Weisz, A.E. Regazzoni, M.A. Blesa, Solid State Ionics 143 (1) (2001) 125–130.
[63] H. Yao, H. Kojima, S. Sato, K. Kimura, Langmuir 20 (23) (2004) 10317–10323.
[64] R.E. Dávila-Martínez, L.F. Cueto, E.M. Sánchez, Surf. Sci. 600 (17) (2006) 3427–3435.
[65] K. Naoi, Y. Ohko, T. Tatsuma, J. Am. Chem. Soc. 126 (11) (2004) 3664–3668.
[66] C. Ryder, M. Byrd, D.J. Wozniak, Curr. Opin. Microbiol. 10 (6) (2007) 644–648.
[67] C. Díaz, P. Schilardi, M.F.L.D. Mele, Artif. Organs 32 (4) (2008) 292–298.
[68] T. Bechert, P. Steinrucke, J.-P. Guggenbichler, Nat. Med. 6 (9) (2000) 1053–1056.

View publication stats